

miR-182-5p and miR-183-5p Act as GDNF Mimics in Dopaminergic Midbrain Neurons

Anna-Elisa Roser,^{1,2} Lucas Caldi Gomes,¹ Rashi Halder,³ Gaurav Jain,³ Fabian Maass,¹ Lars Tönges,⁴ Lars Tatenhorst,¹ Mathias Bähr,^{1,2} André Fischer,^{2,3,5} and Paul Lingor^{1,2}

¹Department of Neurology, University Medical Center Göttingen, Robert-Koch-Str. 40, 37075 Göttingen, Lower-Saxony, Germany; ²DFG Cluster of Excellence Nanoscale Microscopy and Molecular Physiology of the Brain (CNMPB), University Medical Center Göttingen, Robert-Koch-Str. 40, 37075 Göttingen, Lower-Saxony, Germany; ³Department for Epigenetics and Systems Medicine in Neurodegenerative Diseases, German Center for Neurodegenerative Diseases (DZNE), Von-Siebold-Str. 3a, 37075 Göttingen, Lower-Saxony, Germany; ⁴Department of Neurology, Ruhr-Universität Bochum, Universitätsstr. 150, 44801 Bochum, NRW, Germany; ⁵Department of Psychiatry and Psychotherapy, University Medical Center Göttingen, Von-Siebold-Str. 3a, 37075 Göttingen, Lower-Saxony, Germany

Parkinson's disease (PD) is the second-most-frequent neurodegenerative disorder worldwide. One major hallmark of PD is the degeneration of dopaminergic (DA) neurons in the substantia nigra. Glial cell line-derived neurotrophic factor (GDNF) potentially increases DA neuron survival in models of PD; however, the underlying mechanisms are incompletely understood. MicroRNAs (miRNAs) are small, non-coding RNAs that are important for post-transcriptional regulation of gene expression. Using small RNA sequencing, we show that GDNF specifically increases the expression of miR-182-5p and miR-183-5p in primary midbrain neurons (PMNs). Transfection of synthetic miR-182-5p and miR-183-5p mimics leads to increased neurite outgrowth and mediates neuroprotection of DA neurons *in vitro* and *in vivo*, mimicking GDNF effects. This is accompanied by decreased expression of FOXO3 and FOXO1 transcription factors and increased PI3K-Akt signaling. Inhibition of endogenous miR-182-5p or miR-183-5p in GDNF-treated PMNs attenuated the pro-DA effects of GDNF. These findings unveil an unknown miR-mediated mechanism of GDNF action and suggest that targeting miRNAs is a new therapeutic avenue to PD phenotypes.

INTRODUCTION

Parkinson's disease (PD) is the second-most-frequent neurodegenerative disorder worldwide with a yet-unresolved etiology.¹ Although PD is a system disorder affecting different regions of the brain, the progressive demise of the nigrostriatal projections and the inability of this system to regenerate are mainly responsible for the functional motor deficits observed.^{2,3} Studies suggest that gene expression regulators might contribute to a large variety of disease states. MicroRNAs (miRNAs) are endogenous, small, non-coding RNAs that are important for the post-transcriptional regulation of gene expression. Since their discovery, accumulating evidence suggests that they are involved in the regulation of many developmental programs and biological processes and are essential for neuronal development and function.^{4,5} Alterations in miRNA function have been reported in different neurodegenerative diseases, including PD.^{6–9} Furthermore, miRNAs are auspicious therapeutic targets, because the manipulation of their

expression can exert neuroprotection and induce axonal regeneration. However, knowledge on how miRNAs control survival and axonal regeneration in dopaminergic (DA) neurons is limited. Glial cell line-derived neurotrophic factor (GDNF) is one of the most potent pro-DA growth factors that was shown to increase neuronal survival and regeneration in *in vitro* and *in vivo* models of PD.^{10,11} Here, we analyzed the miRNAome of primary midbrain neurons (PMNs) by small RNA sequencing to investigate the effects and mechanism of action of GDNF. Our aim was to identify GDNF-induced changes in miRNA expression that play a role in mediating the pro-DA effects of GDNF. We reveal that GDNF increases the expression of miR-182-5p and miR-183-5p. By employing *in vitro* and *in vivo* approaches, we show that increased levels of these miRNAs mimic GDNF effects in DA neurons. In addition, we demonstrate that inhibition of miR-182-5p or miR-183-5p in GDNF-treated PMN cultures diminishes the beneficial GDNF effects, suggesting that miR-182-5p and miR-183-5p are involved in mediating GDNF effects.

RESULTS

GDNF Specifically Increases miR-182-5p and miR-183-5p Expression in PMNs

We employed small RNA sequencing of PMNs treated with vehicle or GDNF at days *in vitro* (DIV) 1 or 5 (Figure 1A). As expected, we observed substantial changes in miRNA expression when comparing vehicle-treated PMNs at DIV 1 to those at DIV 5 (Figures 1B and 1C). Specifically, 122 miRNAs were differentially expressed at the two developmental stages (Table S1). In contrast, the effect of GDNF treatment on DIV 1 or 5 was more discrete. Only 4 miRNAs were differentially expressed after GDNF treatment in PMNs at DIV 5, among them miR-182-5p and miR-183-5p, with an increased expression (false discovery rate [FDR] = 0.05, log₂ fold change [log₂FC] > 0.5) (Figure 1D).

Received 1 August 2017; accepted 17 January 2018;
<https://doi.org/10.1016/j.omtn.2018.01.005>

Correspondence: Paul Lingor, University Medical Center Göttingen, Robert-Koch-Str. 40, 37075 Göttingen, Lower-Saxony, Germany.

E-mail: plingor@gwdg.de



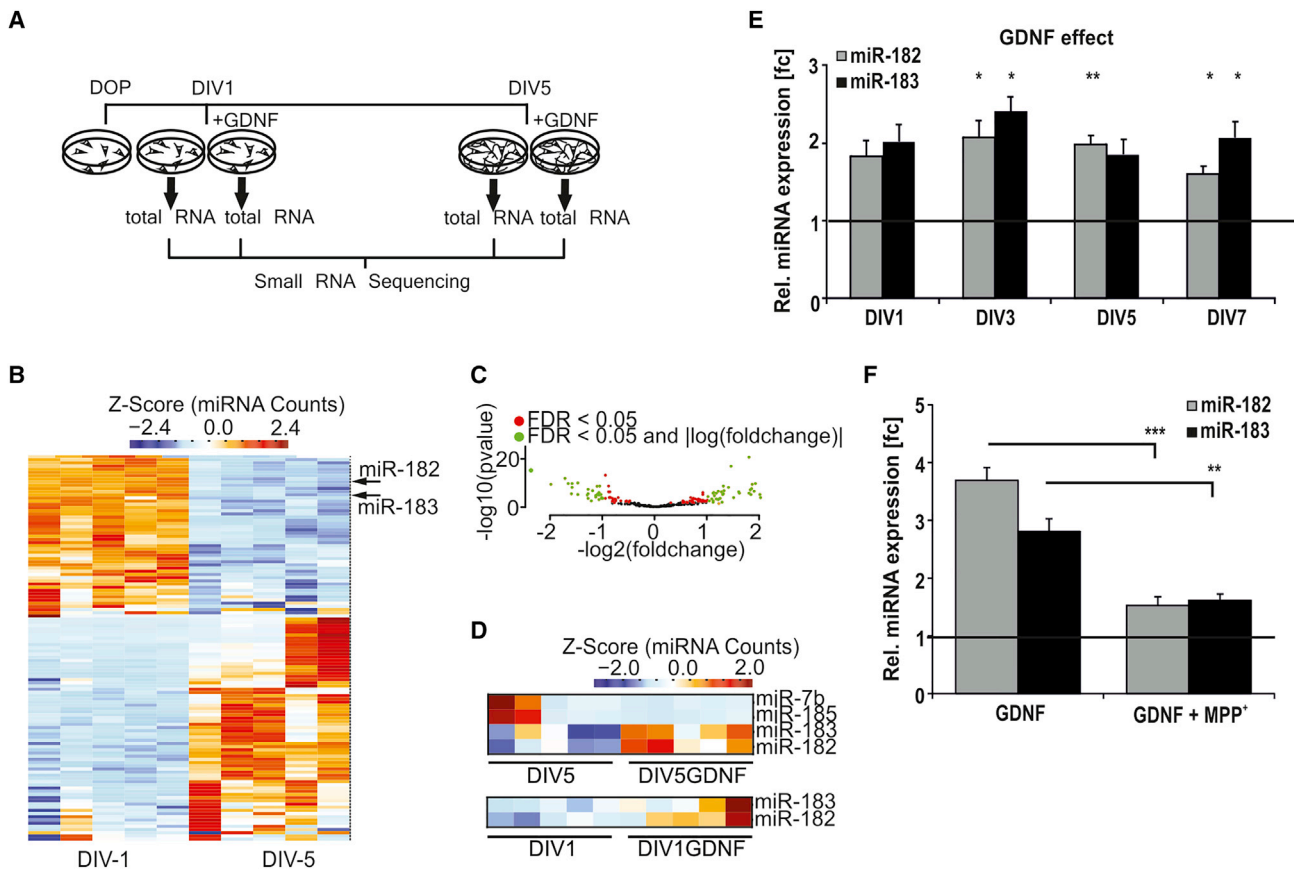


Figure 1. GDNF Increases Expression of miR-182-5p and miR-183-5p in PMNs

(A) Experimental layout for small RNA sequencing. (B) Heatmap showing 122 miRNAs differentially expressed between DIV 1 and DIV 5 (FDR = 0.05, $\log_2\text{FC} = 0.5$). Arrows indicate miR-182-5p and miR-183-5p ($n = 5$ independent cultures). (C) Volcano plot showing all detected miRNAs in DIV 1 and 5 PMNs. Red dots indicate all miRNAs that are significantly different using only FDR as the cutoff. Green dots indicate all miRNAs that are significantly different using FDR and $\log_2\text{FC}$ as the cutoffs. (D) Upper panel: heatmap showing the 4 differentially expressed miRNAs (FDR = 0.05, $\log_2\text{FC} = 0.5$) in vehicle or GDNF-treated PMNs at DIV 5. Lower panel: heatmap showing the expression of miR-182-5p and miR-183-5p after GDNF treatment at DIV 1. (E) Validation of small RNA sequencing results by qRT-PCR ($n = 4$ independent cultures). (F) Expression levels of miR-182-5p and miR-183-5p at DIV 5 in GDNF-treated PMNs after depletion of DA neurons ($n = 5$ independent cultures). Data are presented as mean \pm SEM and were analyzed by unpaired t test. * $p < 0.05$, ** $p < 0.01$, *** $p < 0.001$.

While using the same cutoff, no differentially expressed miRNAs were detected at DIV 1; only miR-182-5p and miR-183-5p showed a non-significant trend for increased expression (Figure 1D). miR-182-5p and miR-183-5p were also among the 122 differentially expressed miRNAs when comparing PMNs at DIV 1 to those at DIV 5 (Figure 1B). Here, miR-182-5p and miR-183-5p decreased at DIV 5. All these findings were confirmed by qRT-PCR, showing that GDNF treatment leads to an upregulation of miR-182-5p and miR-183-5p and suggesting that these miRNAs may play an important role in the plasticity of midbrain neurons (Figure 1E). To assess the question of whether the GDNF-mediated increase in miR-182-5p/miR-183-5p expression is induced in DA neurons or in the γ -aminobutyric acid (GABA)-ergic PMN population as a secondary effect of increased GDNF signaling in DA neurons, we chemically depleted DA neurons by 1-methyl-4-phenylpyridinium (MPP⁺) and subsequently measured miR-182-5p and miR-183-5p expression levels.

MPP⁺ induces a selective DA neuron death in PMN cultures. The depletion of DA neurons by MPP⁺ in GDNF-treated PMN cultures leads to a significant decrease in miR-182-5p and miR-183-5p expression levels compared to non-toxin-treated controls (Figure 1F). This finding indicates that the observed increase of miR-182-5p and miR-183-5p expression in PMNs after GDNF treatment is induced in DA neurons. To gain insight into the role of miR-182-5p and miR-183-5p in midbrain neuron biology, target prediction and functional annotation of the target genes were performed. The results suggest important roles of GDNF-regulated miR-182-5p and miR-183-5p in neuronal biology (Table S2).

Increased miR-182-5p and miR-183-5p Levels Mimic GDNF Effects in DA PMNs

To better understand the role of miR-182-5p and miR-183-5p in DA neurons, PMN cultures were transfected with synthetic miRNA

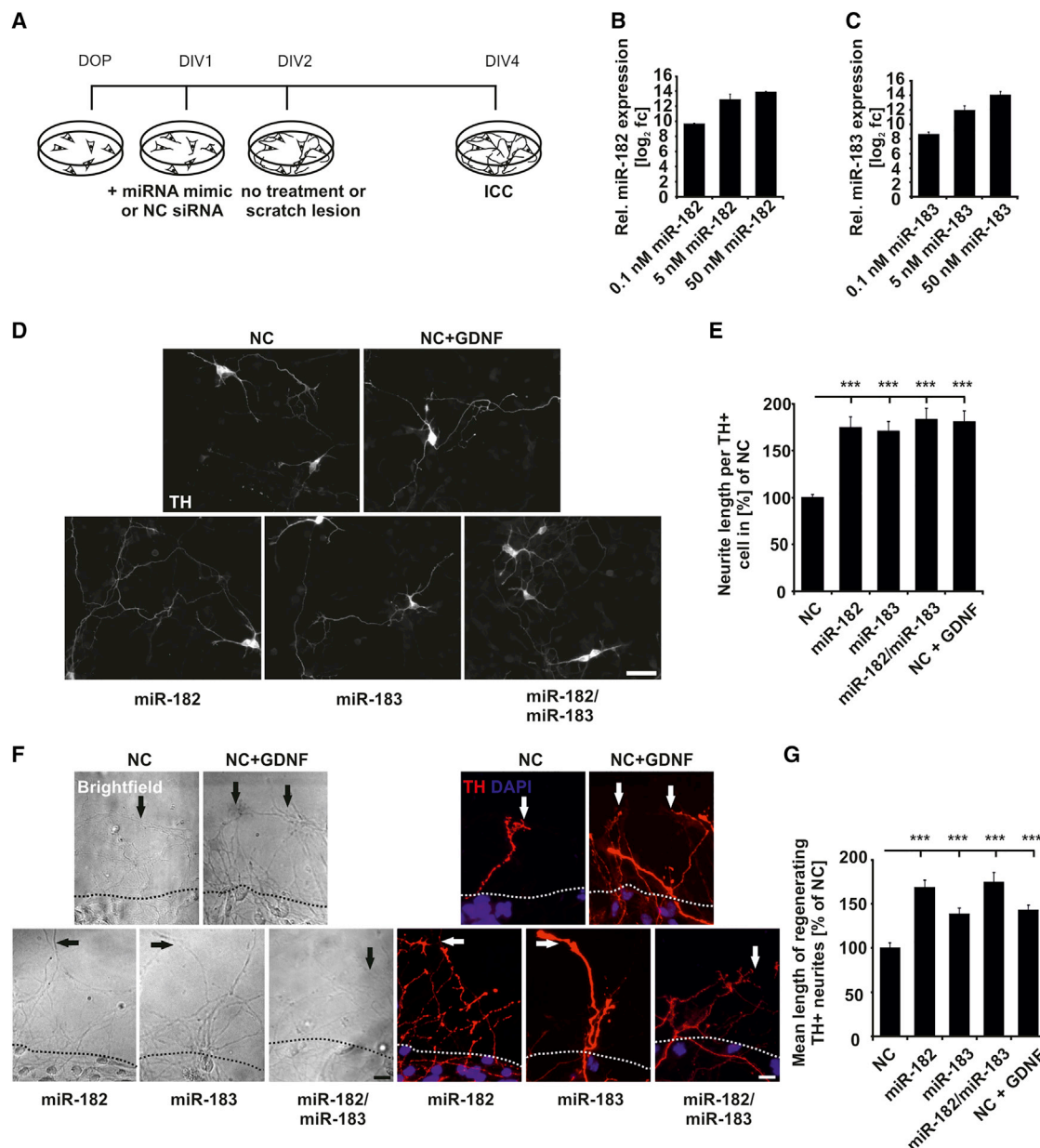


Figure 2. Increased miR-182-5p and miR-183-5p Levels Mimic GDNF Effects on Neurites in PMNs

(A) Experimental layout for neurite growth and regeneration experiments. (B and C) Mature miR-182-5p (B) and miR-183-5p (C) levels in PMNs transfected with different concentrations of the respective mimic 24 hr post-transfection relative to endogenous levels in NC siRNA-transfected PMNs ($n = 3$ independent cultures). (D) Representative micrographs of dopaminergic PMNs transfected with NC, the respective miRNA mimics, or NC and treated with GDNF. PMNs were immunostained against tyrosine hydroxylase (TH) (scale bar, 50 μ m). (E) Quantification of the total neurite length per TH+ cell normalized to NC-transfected cultures ($n = 3$ independent cultures; at least 50 TH+ neurons per culture were analyzed). (F) Right panel: representative micrographs of TH-immunostained and DAPI-counterstained miRNA mimic, NC, or GDNF-treated PMN cultures after mechanical scratch lesion. Left panel: corresponding bright-field images. The scratch border is indicated by the dotted line (scale bar, 10 μ m). (G) Quantification showing the mean length of the 10 longest TH+ neurites crossing the scratch border relative to NC-transfected PMN cultures ($n = 3$ independent cultures). Data are presented as mean \pm SEM and were analyzed by one-way ANOVA with Dunnett's post hoc test. *** $p < 0.001$.

mimics or a scrambled small interfering RNA (siRNA) (negative control [NC] siRNA) (Figures 2B and 2C), and the effects on neurite length, regeneration, and survival of DA PMNs were analyzed (Figures 2, 3A, 3B, 3D, and 3E). Transfection efficiency was analyzed

by qRT-PCR for three mimic concentrations (Figures 2B and 2C) and for all subsequent experiments, 5 nM miRNA mimics were used. For a comparative analysis, PMNs were transfected with NC siRNA and treated with GDNF in a saturating concentration

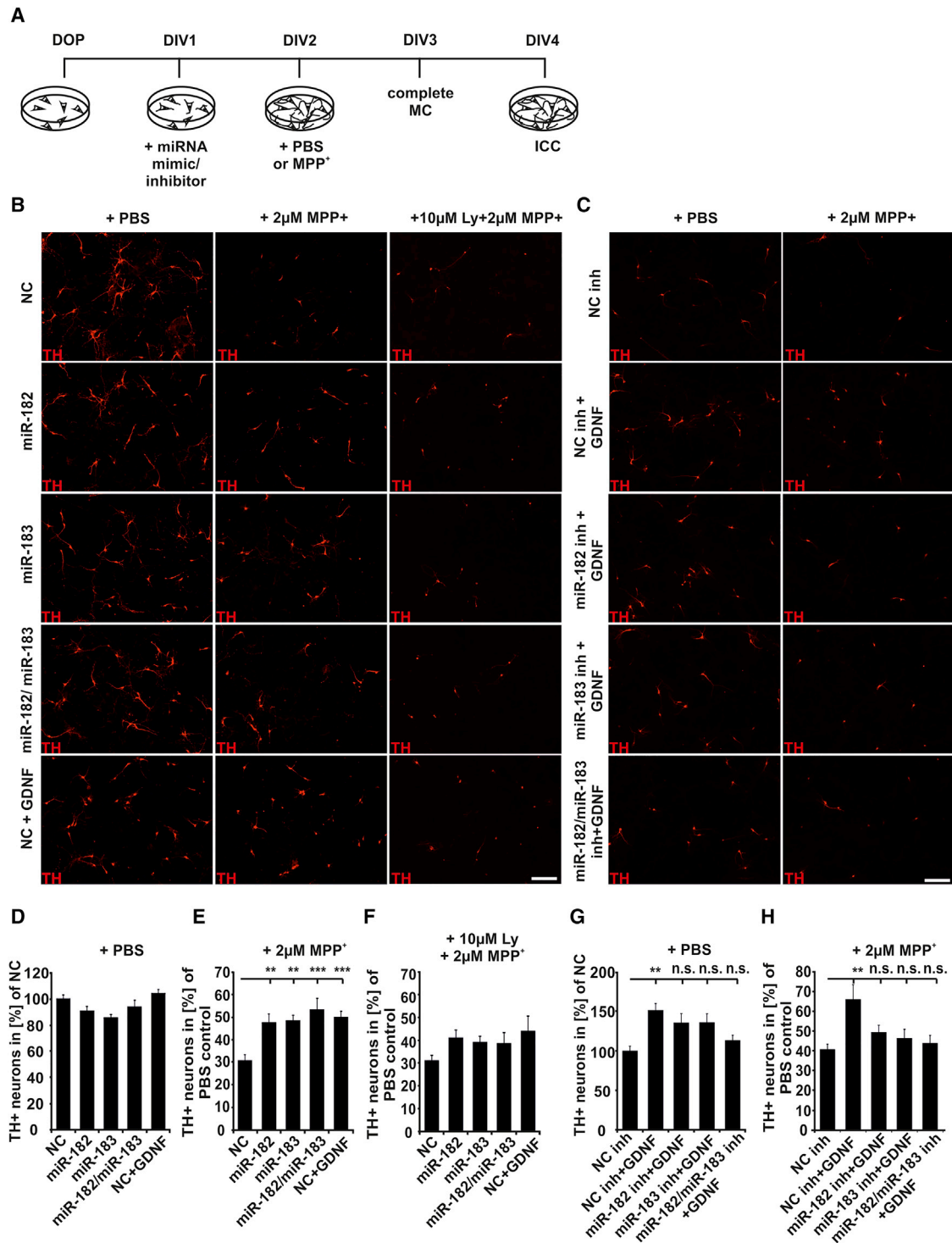


Figure 3. Increased miR-182-5p and miR-183-5p Levels Result in Increased DA Neuron Survival

(A) Experimental layout for MPP⁺ survival experiments. (B and C) Representative micrographs of PMNs treated with (B) miRNA mimics or GDNF after application of PBS (left column), 2 μ M MPP⁺ (for 24 hr) (middle column), or 2 μ M MPP⁺ (for 24 hr) and 10 μ M Ly 294002 (Ly) (for 49 hr, starting 1 hr before MPP⁺ treatment until the end of experiment) (right column) and (C) miRNA inhibitors and GDNF after application of PBS (left column) or 2 μ M MPP⁺ (for 24 hr) (right column). PMNs were immunostained against TH (scale bar, 100 μ m). (D) Quantification of TH⁺ PMNs after transfection with miRNA mimics, NC, or treatment with GDNF and with addition of PBS for 24 hr as an experimental control

(legend continued on next page)

(10 ng/mL). At DIV 4, miR-182-5p- and miR-183-5p-transfected DA PMNs showed a significant increase in neurite length compared to NC siRNA-transfected cultures, and these effects were of comparable magnitude to GDNF treatment (Figures 2D and 2E). To analyze the neuroprotective potential of miR-182-5p and miR-183-5p, the MPP⁺ neurotoxin model was applied, and DA neuron survival was analyzed (Figures 3A, 3B, 3D, and 3E). miRNA mimic transfection without MPP⁺ treatment did not affect DA cell numbers at DIV 4 (Figure 3D). After MPP⁺ treatment, PMNs transfected with miR-182-5p or miR-183-5p mimics showed a significantly higher DA cell survival rate than did NC siRNA-transfected PMNs (Figure 3E). Again, the neuroprotective effect was similar to the effect observed after GDNF treatment (Figure 3E). For a more complete picture of the neuroprotective effects of miR-182-5p and miR-183-5p on DA neuron survival, PMNs without toxin treatment were analyzed at DIV 5 and 7, and DA neuron survival was assessed (Figures S1A and S1B). At DIV 5, no significant increase in DA neuron survival was observed after transfection with miRNA mimics or treatment with GDNF (Figure S1A). Compared to NC siRNA-transfected PMNs, miR-182-5p mimic- and miR-182-5p/miR-183-5p mimic-transfected PMNs show significant higher survival of DA neurons at DIV 7. A similar effect on survival could be observed in GDNF-treated PMNs, but not in miR-183-5p-transfected tyrosine hydroxylase (TH⁺) neurons (Figure S1B).

For the assessment of the pro-regenerative potential of miR-182-5p and miR-183-5p, a mechanical neurite transection was performed and the length of regenerating DA neurites crossing the scratch border was quantified. Compared to NC siRNA, transfection of miR-182-5p and miR-183-5p mimics significantly increased the length of regenerating neurites, which was comparable in the GDNF-treated group (Figures 2F and 2G).

To exclude the possibility that the observed effects are unspecific and only due to increased miRNA levels per se, all experiments were repeated transfecting the heart-specific miR-1a-3p. In previous studies, miR-1a-3p showed no effect on neurite growth in cortical neurons.¹² Transfection of miR-1a-3p had no effect on neurite outgrowth, neurite regeneration, or neuroprotection in PMNs (Figure S2). Thus, the observed findings represent specific effects of miR-182-5p/miR-183-5p transfection.

Inhibition of Endogenous miR-182-5p and miR-183-5p Diminishes the Effects of GDNF in DA PMNs

To gain deeper insight into the interaction of GDNF and miR-182-5p and miR-183-5p in DA PMNs, cells were transfected with locked nucleic acid (LNA) miRNA inhibitors after GDNF treatment. As an NC

inhibitor (NC inh) a validated scrambled LNA oligonucleotide was used, and PMNs treated with GDNF and transfected with NC inh served as a positive control (Figure 4). To verify the function of the miRNA inhibitors, we performed western blots against the miRNA target FOXO1 that is also downregulated upon GDNF treatment. GDNF treatment and transfection with NC inh led to a significant decrease in FOXO1 protein levels. In contrast, GDNF treatment and inhibition of miR-182-5p or miR-183-5p restored FOXO1 protein levels to endogenous levels of GDNF-untreated cells (Figure 4B). The analyses of DA PMN neurite growth showed that transfection with NC inh after GDNF treatment led to a significant increase in neurite length compared to NC inh-transfected PMNs without GDNF treatment. In contrast, transfection of miR-182-5p and miR-183-5p inhibitors after GDNF treatment diminished the GDNF effect on neurite length of DA PMNs (Figures 4C and 4D). To assess the effect of miR-182-5p and miR-183-5p inhibition in GDNF-treated PMNs on DA neuron survival, the MPP⁺ model was applied (Figures 3C, 3G, and 3H). In the PBS-treated experimental control, a significant increase in DA neuron survival in GDNF-treated, NC inh-transfected cultures was observed. This effect was decreased in GDNF-treated PMNs transfected with miR-182-5p and miR-183-5p inhibitors (Figure 3G). In this context and in these experiments, GDNF treatment started with the day of culture preparation—compared to the miRNA mimic experiments, in which the treatment started 3 hr post-transfection—and a GDNF-mediated increase in DA PMN survival in PBS-treated cultures was not observed. After MPP⁺ treatment, NC inh-transfected PMNs treated with GDNF displayed significantly increased DA neuron survival compared to PMN cultures that were maintained without GDNF. The beneficial effect of GDNF was decreased in PMNs transfected with miRNA inhibitors (Figure 3H).

To investigate whether inhibition of miR-182-5p and miR-183-5p also influences the GDNF effect on DA PMN neurite regeneration, a mechanical neurite transection was performed. Although GDNF-treated cultures show a significant increase in DA neurite regeneration, this effect was reduced when miR-182-5p or miR-183-5p was inhibited (Figures 4E and 4F). These results suggest that miR-182-5p and miR-183-5p play a role in mediating the beneficial effects of GDNF on DA PMNs.

miR-182-5p and miR-183-5p Regulate Expression of Foxo Transcription Factors

For the elucidation of miR-182-5p/miR-183-5p-mediated signaling mechanisms, we screened the miRTarBase database¹³ for target genes that had already been experimentally validated and further analyzed

(n = 3 independent cultures). (E) Relative quantification of surviving TH⁺ PMNs after transfection with miRNA mimic, NC, or treatment with GDNF and addition of 2 μ M MPP⁺ (for 24 hr) normalized to PBS-treated cells (n = 3 independent cultures). (F) Relative quantification of surviving TH⁺ PMNs after transfection with miRNA mimic, NC, or treatment with GDNF and addition of 10 μ M Ly (for 49 hr) and 2 μ M MPP⁺ (for 24 hr) normalized to PBS-treated cells (n = 5 independent cultures). (G) Quantification of TH⁺ PMNs after transfection with NC inhibitor, miRNA inhibitor, and/or treatment with GDNF (starting at DIV 0) and addition of PBS for 24 hr as an experimental control (n = 5 independent cultures). (H) Relative quantification of surviving TH⁺ PMNs after transfection with NC inhibitor, miRNA inhibitor, and/or treatment with GDNF (starting at DIV 0) and addition of 2 μ M MPP⁺ for 24 hr normalized to PBS-treated cells (n = 5 independent cultures). Data are presented as mean \pm SEM and were analyzed by one-way ANOVA (D and F) with Dunnett's post hoc test (E, G, and H). **p < 0.01, ***p < 0.001.

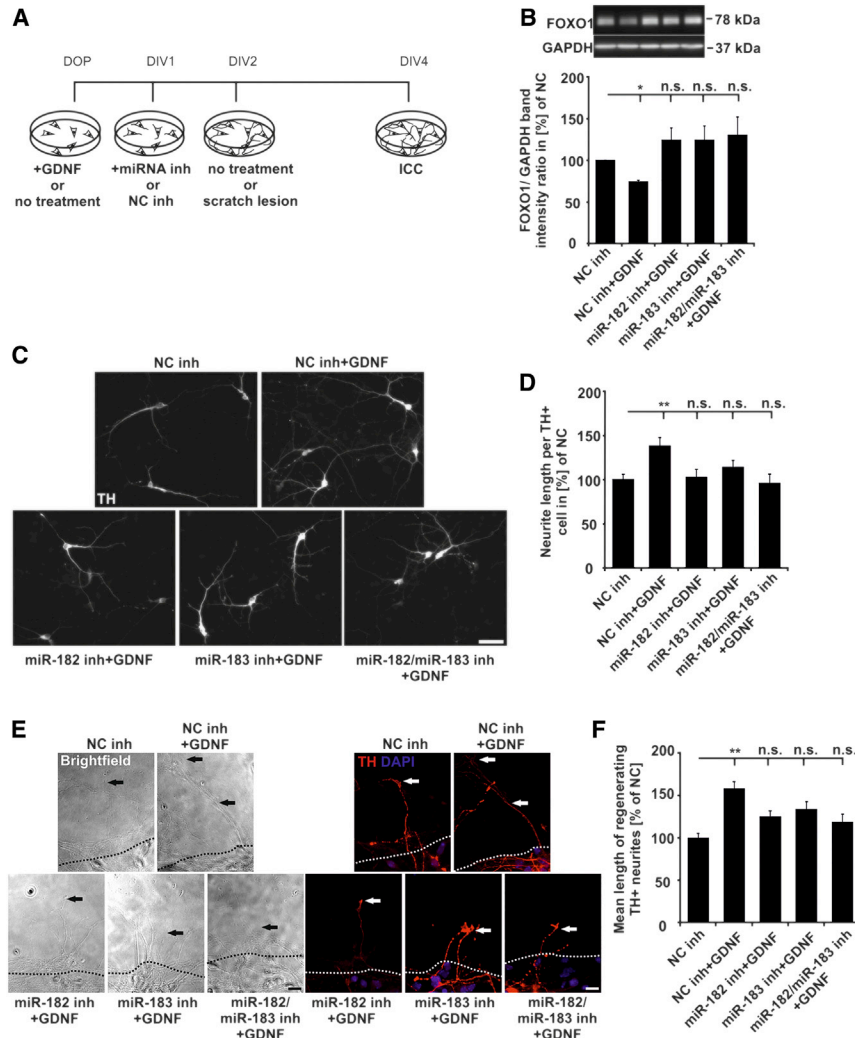


Figure 4. Inhibition of Endogenous miR-182-5p and miR-183-5p Levels Diminishes GDNF Effects on Neurites in PMNs

(A) Experimental layout for neurite growth and regeneration experiments. (B) FOXO1 levels in PMNs transfected with 50 nM of the respective LNA miRNA inhibitor or NC inhibitor and GDNF treatment 48 hr post-transfection relative to endogenous levels in NC inhibitor-transfected PMNs (n = 5 independent cultures). (C) Representative micrographs of dopaminergic PMNs transfected with NC inhibitor, the respective miRNA inhibitor, or NC inhibitor and treated with GDNF. PMNs were immunostained against tyrosine hydroxylase (TH) (scale bar, 50 μ m). (D) Quantification of the total neurite length per TH+ cell normalized to NC inhibitor-transfected cultures (n = 5 independent cultures; at least 30 TH+ neurons per culture were analyzed). (E) Right panel: representative micrographs of TH-immunostained and DAPI-counterstained PMN cultures treated with miRNA inhibitor, NC, or GDNF after mechanical scratch lesion. Left panel: corresponding bright-field images. The scratch border is indicated by the dotted line (scale bar, 10 μ m). (F) Quantification showing the mean length of the 10 longest TH+ neurites crossing the scratch border relative to NC inhibitor-transfected PMN cultures (n = 5 independent cultures). Data are presented as mean \pm SEM and were analyzed by one-way ANOVA with Dunnett's post hoc test. *p < 0.05, **p < 0.01.

thus partly mimicked the effects of GDNF treatment, suggesting that miR-182-5p and miR-183-5p are contributing to the pro-DA effects mediated by GDNF.

To further investigate the role of FOXO1 and FOXO3 in DA PMN survival, PMNs were transfected with FOXO1 or FOXO3 siRNA and DA neuron survival was investigated under the influence of MPP⁺ or in untreated cultures compared to NC siRNA-transfected cultures (Figure S4). siRNA-mediated decrease in FOXO1 and FOXO3 protein levels resulted in increased DA neuron survival in PMN cultures treated with PBS or MPP⁺ (Figures S4C and S4D), supporting the hypothesis that regulation of FOXO1 and FOXO3 protein levels plays a role in mediating miR-182-5p and miR-183-5p mimic effects on DA PMNs. In addition, the importance of PI3K-Akt signaling for mediation of the protective effects of miR-182-5p and miR-183-5p was addressed by analysis of DA neuron survival in MPP⁺-intoxicated PMNs under the influence of a specific inhibitor for PI3K that prevents phosphorylation of Akt, Ly 294002 (Ly). Inhibition of Akt phosphorylation starting 1 hr before MPP⁺ treatment until the end of the experiment diminished the beneficial effect of miR-182-5p and miR-183-5p on DA neuron survival in PMN cultures (Figures 3B and 3F).

In conclusion, the observed miRNA effects on neurite outgrowth, neurite regeneration, and survival of DA neurons appear to be

the FOXO3 and FOXO1 transcription factors. Both have been previously shown to be targeted by miR-182-5p^{14,15} and are known to be involved in the induction of neuronal apoptosis upon oxidative stress and interference with neurite growth.^{16–19} FOXO1 is also a predicted target of miR-183-5p in mice (TargetScan 6.2). Transfection of PMNs with miR-182-5p mimics was accompanied by a significant decrease in FOXO3 and FOXO1 expression (Figures 5A and 5B). FOXO1 was also decreased in miR-183-5p-transfected PMNs, validating a previously predicted miRNA-target gene interaction. In addition, increased miR-182-5p and miR-183-5p levels resulted in significantly upregulated phosphatidylinositol 3-kinase (PI3K)-Akt signaling, shown by increased phosphorylated Akt (pAkt) levels, and increased phosphorylation of S6 (Figures 5C–5E). GDNF increased Akt phosphorylation by trend (p = 0.06) and resulted in significantly higher phosphorylation of S6 (Figures 5D and 5E). Increased mitogen-activated protein kinase (MAPK)-pathway activation was shown for GDNF-treated PMNs, but not for miR-182-5p and miR-183-5p mimic-transfected cells (Figure S3). The effect of miRNA increase

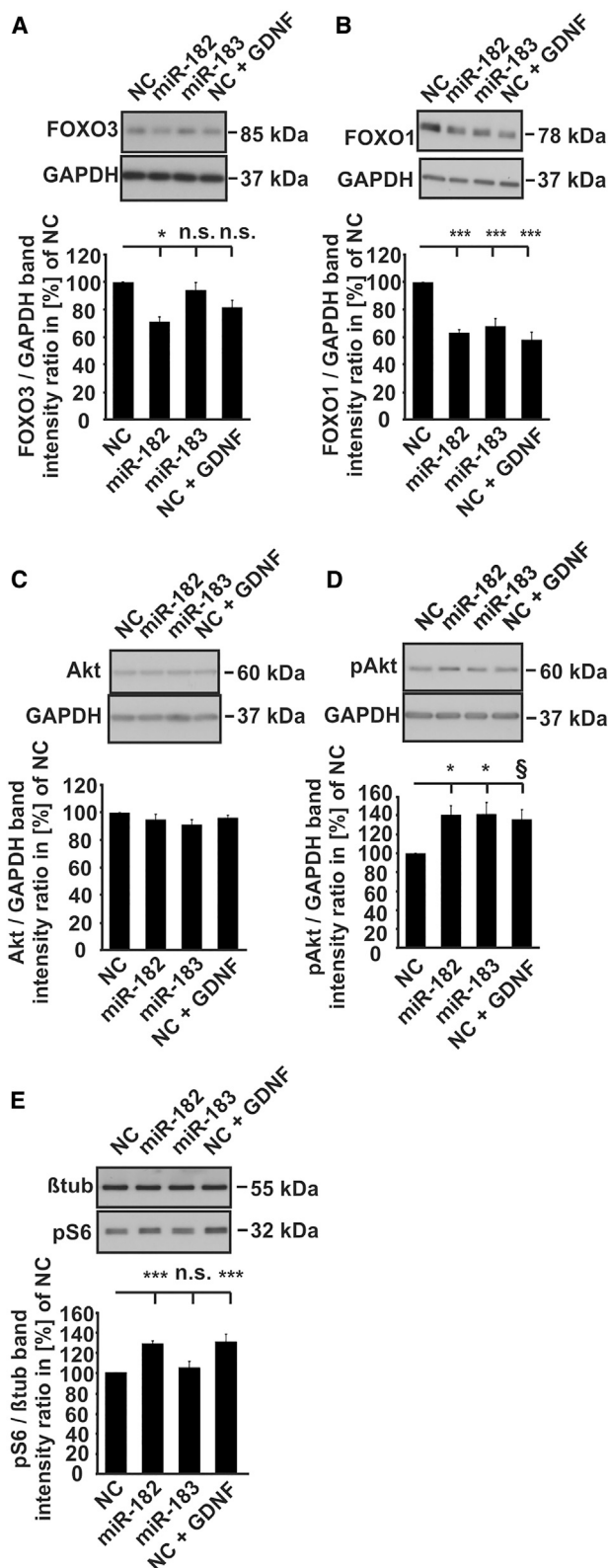


Figure 5. miR-182-5p/miR-183-5p Regulate Expression of FOXO Transcription Factors and Activate PI3K-Akt Signaling

(A–E) Western blot analyses for (A) FOXO3 ($n = 5$ independent experiments [NC + GDNF, $n = 3$]), (B) FOXO1 ($n = 4$ independent experiments [NC + GDNF, $n = 3$]), (C) Akt ($n = 6$ independent experiments [NC + GDNF, $n = 3$]), (D) pAkt ($n = 6$ independent experiments [NC + GDNF, $n = 3$]), and (E) phospho-S6 (pS6) ($n = 5$ independent experiments). Data are presented as mean \pm SEM and were analyzed by one-way ANOVA with Dunnett's post hoc test. * $p < 0.05$, *** $p < 0.001$, § $p = 0.06$.

mediated by a decrease in FOXO3 and FOXO1 transcription factors and increased activation of survival signaling via the PI3K-Akt pathway.

Transfection with miR-182-5p or miR-183-5p Leads to Increased Nuclear Translocation of Sp1 in PMNs

To clarify how GDNF, miR-182-5p, and miR-183-5p mediate their effects and how GDNF regulates the expression of the miRNAs, we investigated the nuclear levels of the transcription factor Sp1. Sp1 has been previously shown to mediate the expression of miR-182-5p/miR-183-5p and has putative binding sites in the GDNF promoter.^{20–23} There is evidence that activation of the PI3K-Akt pathway leads to increased transcriptional activity of Sp1.²⁴ PMNs were transfected with miRNA mimics of NC siRNA, and nuclei were isolated by subcellular fractionation (Figures 6A and 6B). Transfection of PMNs with miR-182-5p or miR-183-5p resulted in significantly increased levels of nuclear Sp1 compared to PMNs transfected with NC siRNA (Figure 6C). GDNF treatment of PMNs transfected with the NC siRNA resulted in a comparable increase in nuclear Sp1 levels (Figure 6C), supporting the hypothesis that GDNF upregulates miR-182-5p and miR-183-5p expression by increased nuclear translocation of Sp1 (Figure 6D).

miR-182-5p Mediates Nigrostriatal Protection in the MPTP Mouse Model of PD

After demonstrating the beneficial effects of GDNF-regulated miR-182-5p and miR-183-5p on DA neurons *in vitro*, we investigated the effect of these miRNAs on DA neurons in the substantia nigra (SN) *in vivo* using the 1-methyl-4-phenyl-1,2,3,6-tetrahydropyridine (MPTP) mouse model of PD. First, we demonstrated the successful transfection of DA neurons in the SN by injection of fluorescently labeled siRNA ($84\% \pm 1\%$ of TH+ neurons were transfected 48 hr post-injection) (Figure 7A). Animals received a stereotactic injection of miR-182-5p/miR-183-5p mimics or NC siRNA into the right SN and were treated with MPTP for 5 consecutive days (Figures 7D and 8A). Compared to animals injected with the NC siRNA, nigral injection of miR-182-5p led to significant morphological preservation of DA cell bodies and, to a lesser extent, their nigrostriatal projections after MPTP lesion (Figures 7E–7I). This was accompanied by increased striatal dopamine levels in miR-182-5p-injected animals (Figure 8B), whereas striatal 3,4-dihydroxyphenylacetic acid (DOPAC) and homovanillic acid (HVA) levels remained unchanged (Figures 8C and 8D). Injection of miR-183-5p mimics led to a similar, but not significant, trend. Furthermore, the

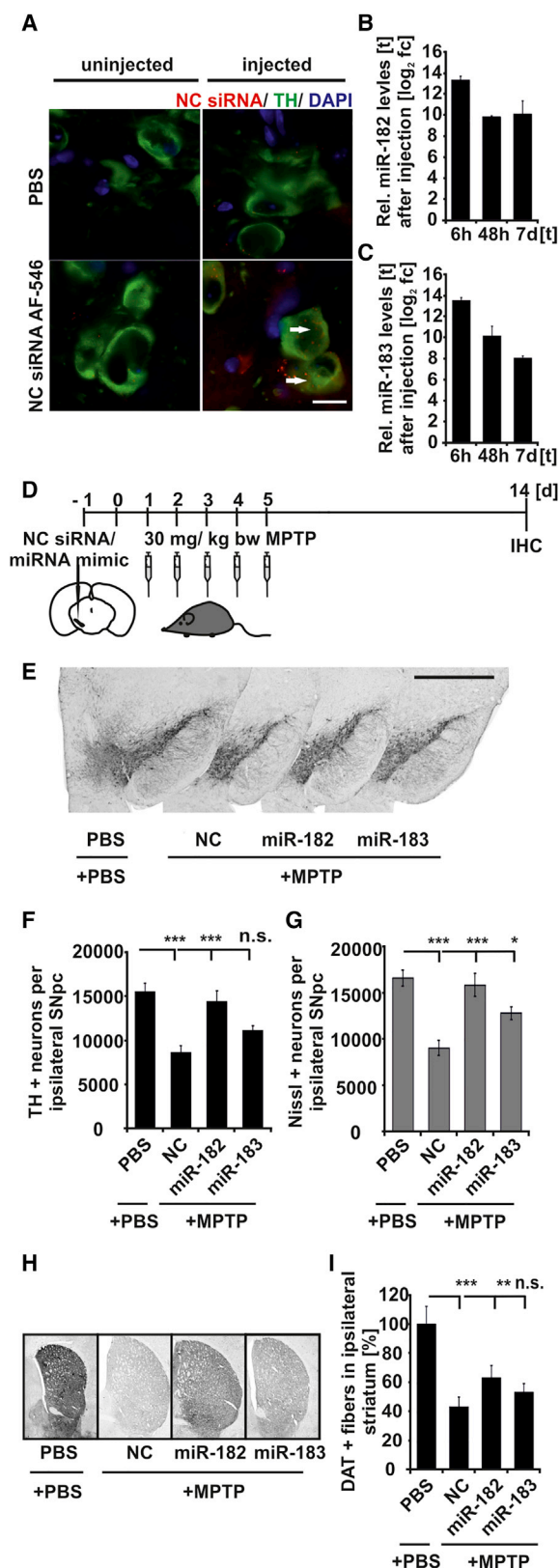


Figure 7. Effects of Increased miR-182-5p/miR-183-5p Levels on the DA Nigrostriatal System in the MPTP Mouse Model of PD

(A) Representative micrographs of SN of Alexa Fluor 546 (AF-546)-labeled NC siRNA-injected animals (left panel, uninjected side; right panel, injected side; scale bar, 20 μ m). (B and C) Relative miR-182-5p (B) and miR-183-5p (C) levels in the midbrain at indicated time points after injection of miRNA mimics (n = 3 animals per condition). (D) Experimental layout of *in vivo* experiments. (E) Exemplary micrographs of the ipsilateral SN. (F) Results of the stereological quantification showing the numbers of TH+ DA neurons per ipsilateral SN (n = 6 animals per group [PBS, n = 5]). (G) Stereological quantification of Nissl+ neuronal cells in the ipsilateral SN (n = 6 animals per group [PBS, n = 5]). (H) Representative micrographs of the ipsilateral striatum stained for dopamine transporter (DAT). (I) Quantification of DAT+ striatal fiber density relative to PBS control animals (n = 6 animals per group [PBS, n = 5]). Data are presented as mean \pm SEM (C) and were analyzed by one-way ANOVA with Dunnett's post hoc test (F, G, and I). *p < 0.05, **p < 0.01, ***p < 0.001.

183-5p in DA neurons has not been published. However, they have been reported to exert important functions in sensory neurons³⁰ and memory formation.³¹ In addition, miR-182-5p and miR-183-5p are necessary for proper function and maintenance of the retina.³² A study in cortical neurons showed that miR-182-5p regulates neurite outgrowth via activation of the PI3K-Akt pathway.³³ Our results also show increased activation of the PI3K-Akt pathway after increase of miR-182-5p and miR-183-5p in PMNs, and a similar trend could be observed in NC siRNA-transfected cultures treated with GDNF. The importance of PI3K-Akt signaling was underlined by Akt inhibition in MPP⁺-treated cultures, diminishing the beneficial effects of both miRNAs and GDNF on DA neuron survival in PMN cultures.

Similar to GDNF treatment, the increase of both miR-182-5p and miR-183-5p leads to decreased expression of FOXO1, and increased miR-182-5p levels resulted in downregulation of the levels of FOXO3 protein, another member of the FOXO transcription factor family. By applying siRNA against FOXO1 and FOXO3, the beneficial effects of decreased FOXO1 and FOXO3 protein levels were confirmed in DA PMNs, indicating the relevance of the miR-FOXO1/FOXO3 target pair for the observed results. This is in line with previous studies reporting that inhibition of FOXO1 and FOXO3 transcription factors plays a role in neurite growth and regeneration, as well as prevention of apoptosis upon oxidative stress in different models.^{18,19,34–36} Altogether, these results indicate that the observed effects of miR-182-5p and miR-183-5p increase in DA PMNs are at least partially mediated by activation of the PI3K-Akt signaling pathway and downregulation of FOXO transcription factors.

Transfection of miR-182-5p and miR-183-5p mimics, as well as GDNF treatment, leads to increased nuclear translocation of the transcription factor Sp1. The effects of increased nuclear translocation of Sp1 in DA PMNs have not been described yet, but increased Sp1 activation has been reported to prevent neuronal death upon oxidative stress in cortical neurons.³⁷

The results of the PMN study indicated that miR-182-5p and miR-183-5p exert pro-DA effects and partially mediate the effects

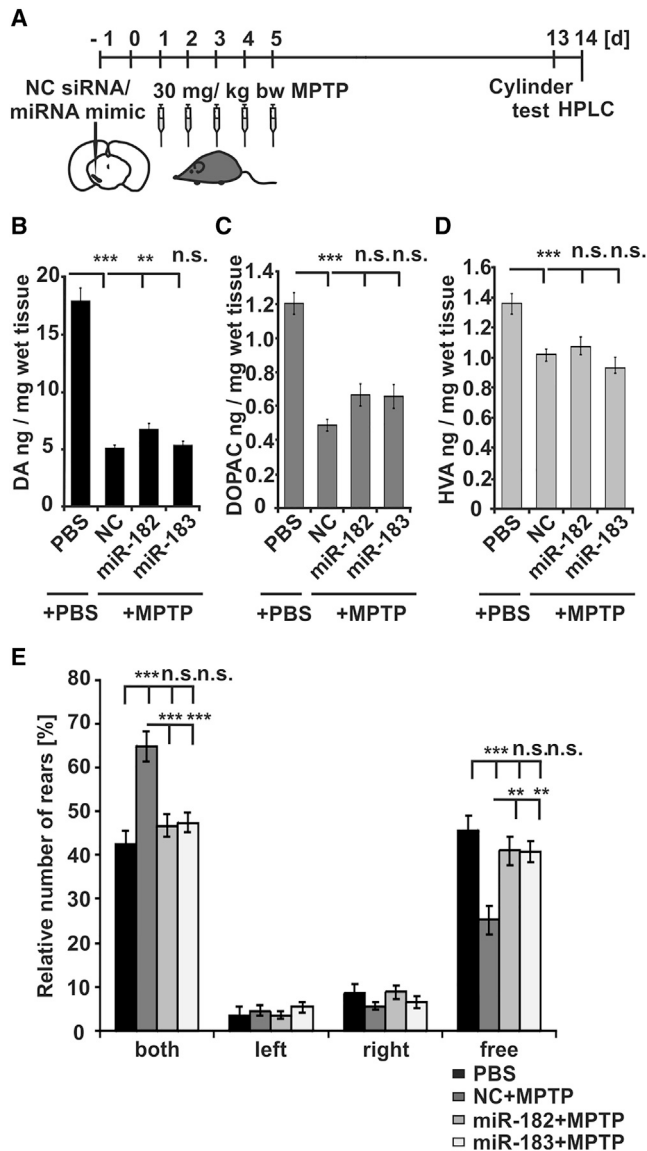


Figure 8. Effects of Increased miR-182-5p and miR-183-5p Levels on the Striatal DA Content and Motor Behavior in the MPTP Mouse Model of PD (A) Experimental layout of *in vivo* experiments. (B–D) Quantification of striatal DA (B), 3,4-dihydroxyphenylacetic acid (DOPAC) (C), and homovanillic acid (HVA) (D) contents in the ipsilateral striatum of experimental animals by HPLC (PBS, $n = 5$ animals; NC, $n = 9$ animals; miR-182, $n = 8$ animals; miR-183, $n = 9$ animals). (E) Quantification of explorative rearing behavior in the cylinder test showing the proportion of rears the animals performed with the aid of both front paws (both), the left paw (left), the right (right) paw, or without the use of their front paws (free) (PBS, $n = 5$ animals; all other groups, $n = 15$ animals). Data are presented as mean \pm SEM and were analyzed by one-way ANOVA with Dunnett's post hoc test. ** $p < 0.01$, *** $p < 0.001$.

of GDNF in DA PMNs. To verify the validity of these results *in vivo*, we studied the effects of increased levels of miR-182-5p and miR-183-5p in the MPTP mouse model of PD. Compared to NC siRNA-injected animals, miR-182-5p mimic-injected animals

show significantly increased survival of DA neurons in the SN, increased striatal DA fiber density, and higher striatal DA content. miR-183-5p-injected and MPTP-intoxicated animals show a significant increase in total neuronal cell numbers compared to NC siRNA-injected mice. These findings are accompanied by restored MPTP-induced behavioral deficits in the cylinder test after miR-182-5p and miR-183-5p mimic injection. The neuroprotective effects of miR-182-5p mimic injection on SN DA neurons in the MPTP mouse model are comparable to previously published effects of nigral GDNF injection.³⁸ The observation that injection of miR-182-5p and (with limitations) miR-183-5p mimics leads to beneficial effects in the MPTP-mediated DA neuron lesion model provides further evidence for the neuroprotective effects of these miRNAs.

This study did not address in detail the mechanism of GDNF-mediated upregulation of miR-182-5p and miR-183-5p expression. However, a possible explanation for the GDNF-dependent increase in miR-182-5p and miR-183-5p expression could be the activation of Sp1, a transcription factor that mediates the expression of miR-182-5p/miR-183-5p in different cell types and that has putative binding sites in the GDNF promoter.^{20–23} Furthermore, it has been shown that Sp1 can act downstream of the PI3K-Akt pathway.^{39–41} In the present study, we show that increased levels of miR-182-5p and miR-183-5p result in higher activation of the PI3K-Akt pathway in PMNs. Increased nuclear translocation of Sp1 after transfection with miR-182-5p or miR-183-5p mimics, as well as upon treatment with GDNF, has been shown in PMNs. We hypothesize that this nuclear translocation leads to induction of SP1-mediated gene expression, which in turn might result in increased miR-182-5p and miR-183-5p expression upon GDNF treatment (Figure 5D). Favoring this hypothesis is the finding that FOXO1 inhibits the transcriptional capacity of Sp1, as was shown in hepatocytes.⁴² Thus, a miR-182-5p/miR-183-5p-mediated decrease in FOXO1 might lead to increased transcriptional activity of Sp1.

Our data indicate a potential of miR-182-5p/miR-183-5p for improving survival and regeneration of DA neurons, which is of interest for the treatment of PD, even if a more complete assessment of the therapeutic potential of miR-182-5p/miR-183-5p mimics will require further studies on the mechanism of action and verification in transgenic animal models of PD. The major challenges in synthetic miRNA-based therapeutics are targeted cell- or tissue-specific delivery while preventing the introduction of supraphysiological miRNA levels. Next to viral vector-based approaches, possible strategies include conjugation with targeting molecules or encapsulation to enhance cell-specific uptake. Similar to previous attempts to deliver GDNF, microcatheter placement for local application could also be discussed.⁴³ Our results thus establish a previously undescribed link between GDNF and miR-182-5p/miR-183-5p and propose both miRNAs as putative therapeutic targets for neurodegenerative disorders with DA demise, such as PD.

MATERIALS AND METHODS

Cell Culture, Transfection of miRNA Mimics, and Assays for Neurite Growth and Neuroprotection

PMNs were prepared under serum-free conditions from embryonic day 12.5 (E12.5) C57BL/6J mice as previously described.⁴⁴ PMN cultures used in this study contain on average ~6% DA neurons and ~94% GABAergic neurons, with only single glial fibrillary acidic protein-positive cells being detectable during the culture time. At DIV 1, PMNs were transfected with synthetic miRNA mimics (miScript miRNA mimics, QIAGEN, Hilden, Germany) for mmu-miR-182-5p (5'-UUUGGCAAUGGUAGAACUCACA CCG-3'), mmu-miR-183-5p (5'-UAUGGCACUGGUAGAAUUC ACU-3'), or mmu-miR-1a-3p (5'-UGGAAUGUAAAGAAGUAUG UAU-3') for dose finding with 0.1, 5, and 50 nM (all other experiments with 5 nM) using HiPerfect (QIAGEN) as a transfection reagent according to manufacturer's instructions. The latter was used as a miRNA control to make sure that the observed effects are not a result of increased miRNA levels per se. As experimental control, we used a validated scrambled NC siRNA (NC; All Stars Negative Control siRNA, QIAGEN) that has no homology to any known mammalian gene. To investigate the effect of inhibition of mmu-miR-182-5p and mmu-miR-183-5p, DIV 1 PMN cultures were transfected with 50 nM LNA miRNA inhibitors (miRCURY LNA Inhibitors, Exiqon, Vedbaek, Denmark) for mmu-miR-182-5p (miR-182-5p inh; 5'-TGTGAGTTCTACCATTGCCAA-3') or mmu-miR-183-5p (miR-183-5p inh; 5'-AGTGAATTCTACCAG TGCCAT-3') using HiPerfect transfection reagent and a LNA negative control inhibitor (NC inh; miRCURY LNA Inhibitor Control, Negative Control A, Exiqon; 5'-TAACACGTCTATACGCCCA-3') as an experimental control. For comparison with the effect of GDNF treatment, we included an experimental group in which cells were transfected with NC siRNA/LNA NC inh and treated with GDNF (PeproTech, Hamburg, Germany) at a final concentration of 10 ng/mL (GDNF treatment starting after the transfection for mimic experiments and after plating for inhibitor experiments). For investigation of neuroprotective effects of miR-182-5p/miR-183-5p, transfected PMNs were treated with 2 μ M of MPP⁺ (Sigma-Aldrich, Taufkirchen, Germany) for 24 hr beginning at DIV 2. To assess the effect of Akt inhibition on DA PMN survival after MPP⁺ treatment, 10 μ M of Ly (CST, Leiden, the Netherlands), a highly specific inhibitor of PI3K that blocks PI3K-dependent Akt phosphorylation, was added to the cell culture medium 1 hr before MPP⁺ treatment. Ly treatment continued until the end of the experiment (49 hr in total). For assessment of neurite regeneration, a mechanical transection of neurites was performed at DIV 2. Neurite growth, regeneration, and survival (after MPP⁺) of DA TH⁺ PMNs were assessed at DIV 4. Survival of DA neurons without toxin was assessed at DIV 5 and 7.

To investigate the effect of decreased FOXO1 and FOXO3 protein levels on DA PMN survival, PMNs were transfected with 50 nM of FOXO1 siRNA (FlexiTube siRNA Mm_FOXO1_4; Mm_FOXO3_2, QIAGEN) or NC siRNA at DIV 1; subsequently, the MPP⁺ model was applied as described earlier.

For investigation of DA neurite length, neuronal survival, and neurite regeneration, PMNs on glass coverslips immunolabeled against TH were imaged with a Zeiss Axioplan microscope equipped with a 16-bit grayscale charge-coupled device (CCD) camera using the 20 \times objective and AxioVision SE64 4.9.1 software with the MosaiX module (Zeiss, Jena, Germany). Per transfection experiment, at least two independent transfections per culture were performed, and experiments were replicated at least three times. Per coverslip, two 2.1 mm² areas (20 images at 20 \times magnification) were randomly imaged and analyzed. All images in one experiment were acquired with the same exposure time, and for analyses, the same color intensities were used. Images were analyzed using ImageJ 1.48 software (NIH, Bethesda, Maryland, USA). For analyses of DA neurite length and regeneration, the NeuronJ macro was applied. For neurite regeneration, the 10 longest TH⁺ neurites along the scratch border per 2.1 mm² area were analyzed in at least 3 areas per experiment. DA cell bodies in the MPP⁺ experiments were counted using the CellCounter tool.

Small RNA Sequencing, Reverse Transcription, and Real-Time qPCR

Small RNA sequencing was performed on an Illumina HiSeq 2000 system. Total RNA was isolated from PMNs at different time points and after GDNF treatment using TRI reagent. Small RNA libraries were prepared from 1 μ g total RNA using the Illumina TruSeq Small RNA Sample Preparation Kit (San Diego, California, USA). For processing of sequencing data, a customized, in-house software pipeline was used. Quality check and demultiplexing were performed using the CASAVA 1.8.2 software (Illumina). We trimmed the 3' adapters and filtered out the reads with the minimum length of 15 nucleotides using cutadapt. We first mapped the reads to the reference genome created from miRNA sequences. Remaining unmapped reads were then mapped to the human genome. All mapping was performed using rna-STAR. We allowed no mismatches for the reads < 25b, one mismatch for reads between 26b and 33b, two mismatches for reads between 33b and 59b, and so on. We mapped all reads in the non-splice-junction-aware mode. For comparison of miRNA expression between samples, a differential expression analysis was performed using R DESeq2 and the RUVseq package. Small RNA sequencing data are accessible at GEO: GSE109066. Heatmaps were created using custom python script for python v.2.7.1 and Matplotlib 1.5.1. Computational miRNA target prediction analysis was performed using TargetScanMouse 6.2.⁴⁵ Predicted miRNA target genes were functionally annotated using the data mining environment provided by the DAVID platform.⁴⁶ The functional annotation module was applied for gene ontology terms using an Expression Analysis Systemic Explorer (EASE) score of 0.1 and a minimum number of 2 counts. Enrichment of miRNA targets in specific Kyoto Encyclopedia of Genes and Genomes (KEGG) pathways using DIANA miRPath was employed.⁴⁷ Already experimentally validated target genes were searched using the miRTarBase database.¹³ FOXO1 and FOXO3 were chosen as miRNA targets for further analyses as follows. First, experimentally validated targets for mmu-miR-182-5p and mmu-miR-183-5p were searched using miRTarBase. This resulted

in 9 experimentally validated targets for mmu-miR-182-5p and 4 experimentally validated targets for mmu-miR-183-5p that were validated with methods giving strong evidence (among them FOXO3 for miR-182-5p). For comparison, we also looked for experimentally validated targets for hsa-miR-182-5p and hsa-miR-183-5p, respectively, and found that FOXO1 (for both miRNAs) and FOXO3 (for miR-182-5p) were experimentally validated targets (high evidence). Comparison of these findings with predicted targets for mmu-miR-183-5p showed that FOXO1 is also a predicted target for miR-183-5p in mice. Because FOXO transcription factors are reported to play an important role in induction of neuronal apoptosis, we decided to investigate them further as targets for miR-182-5p and miR-183-5p in our model.

For real-time qPCR, total RNA was isolated from PMNs treated with vehicle or GDNF at indicated time points. To deplete DA neurons in the PMN cultures, cells were treated with 5 μ M MPP⁺ for 48 hr beginning at DIV 3 (RNA isolated at DIV 5). cDNA synthesis from total RNA was performed using the miScript II RT kit (QIAGEN), and miRNA expression levels were determined by real-time qPCR in the CFX96 Touch Real-Time PCR Detection System (Bio-Rad, Munich, Germany) using the miScript SYBR Green PCR Kit (QIAGEN) and mature miRNA-specific primers (Mm_miR-182_2 miScript Primer Assay, Mm_miR-183_1 miScript Primer Assay, and Mm_miR-1_2 miScript Primer Assay, QIAGEN). miRNA expression was normalized to the endogenous control RNU6 (Hs_RNU6-2_11 miScript Primer Assay, QIAGEN) in a reaction volume of 15 μ L and under cycling conditions according to manufacturer's instructions.

SDS-PAGE and Immunoblotting

To study the expression levels of miR-182-5p and miR-183-5p targets FOXO1 and FOXO3, as well as activation of survival- and growth-associated pathways, western blotting was performed. Protein lysates were prepared from PMNs 24 hr post-transfection as previously reported.^{3,48} For investigation of nuclear Sp1 levels, nuclei of PMNs were isolated by subcellular fractionation as previously reported.⁴⁹

Western blotting was performed with 20 μ g of protein using the following primary antibodies: monoclonal rabbit anti-FOXO1, 1:500; monoclonal rabbit anti-FOXO3, 1:500; polyclonal rabbit anti-Akt, 1:1,000; polyclonal rabbit anti-phosphorylated Akt, 1:1,000; and polyclonal rabbit anti-phosphorylated S6 ribosomal protein (phosphor-S6 [pS6]), 1:1,000 (Cell Signaling Technology, Cambridge, UK); polyclonal rabbit anti-Sp1 (PEP2), 1:100 (Santa Cruz Biotechnology, Dallas, Texas, USA); polyclonal rabbit anti-Lamin B1-nuclear envelope marker, 1:1,000 (Abcam, Cambridge, UK); monoclonal mouse anti-Gapdh 1:2,000 (HyTest, Turku, Finland); and monoclonal mouse anti- β -tubulin, 1:5,000 (Sigma-Aldrich). This was followed by incubation with the corresponding horseradish peroxidase-coupled secondary antibody (goat anti-rabbit or goat anti-mouse, 1:2,000; Cell Signaling Technology). For detection of protein bands, the membrane was incubated with a reagent for enhanced chemiluminescence for 1 min and either exposed to

autoradiography films, which were developed in a Curix 60 Developer, or imaged with a Fusion Pulse 6 imaging system.

Stereotactic Injection of Oligonucleotides and MPTP Treatment

For stereotactic injections of synthetic miRNA mimics into the right SN of mice, the animals were anesthetized, the scalp was disinfected, and a longitudinal cut along the midline was executed to expose bregma and lambda. The coordinates for an injection in the right SN relative to bregma were set (anterior-posterior [AP], -0.29 cm; mediolateral [ML], -0.12 cm; dorsal-ventral [DV], -0.45 cm^{50,51}), and 2 μ L of oligonucleotide solution prepared as previously reported⁸ was injected.

To investigate the neuroprotective effect of increased miR-182-5p and miR-183-5p levels, animals received intraperitoneal injections of 30 mg/kg body weight MPTP or PBS (for controls) on 5 consecutive days³ beginning 48 hr after the nigral stereotactic injection of the oligonucleotide. Animals were sacrificed at day 14 after the first MPTP injection. All animal experiments were carried out according to the regulations of the local animal research council and legislation of the State of Lower Saxony, Germany (G13/1118).

Histology and Neurochemical Analyses

For stereological evaluation of DA neuron numbers in the SN, midbrain sections were immunostained against TH, followed by a Nissl staining.^{3,48} The number of DA (TH+) neurons and the total number of neurons (Nissl-positive cells) in the ipsilateral SN were analyzed by counting every 4th 3,3'-diaminobenzidine (DAB)-stained section over the whole SN using Stereo Investigator software (Micro Bright Field).

For analysis of striatal fiber density, striatal sections were stained against dopamine transporter (DAT). Every 4th DAT-stained section over the whole striatum was imaged and analyzed using ImageJ 1.48. Five sections per animal were analyzed.

For neurochemical analysis of dopamine and its metabolites in the striatum, homogenates were prepared from fresh, unfixed tissue. Striatal dopamine, DOPAC, and HVA were quantified by high-performance liquid chromatography (HPLC) as previously reported.^{3,48}

Analysis of Rearing Behavior

To evaluate potential changes in motor behavior after miRNA mimic injection in the MPTP mouse model, forelimb use during natural exploratory behavior was assessed using the cylinder rearing test.⁵²

Statistical Analysis

Statistical analysis was performed with KyPlot v.2.0 (KyensLab) and SigmaPlot v.11 (Systat Software). Data are given as mean \pm SEM. The statistical test and the number of experiments or animals used for analysis are indicated in the respective figure legends. No data points were removed from statistical analyses. In all experiments, no statistical methods were used to predetermine sample sizes, but sample sizes are similar to those routinely used in the field for these

experiments. Differences were considered significant with $p < 0.05$ (* $p < 0.05$, ** $p < 0.01$, *** $p < 0.001$).

SUPPLEMENTAL INFORMATION

Supplemental Information includes four figures and two tables and can be found with this article online at <https://doi.org/10.1016/j.omtn.2018.01.005>.

AUTHOR CONTRIBUTIONS

A.-E.R. contributed to the design of the study and its experiments, performed the experiments, analyzed and interpreted the data, and wrote the paper. L.C. was involved in western blotting experiments and participated in the revision experiments. R.H. performed the small RNA sequencing and revised the manuscript. G.J. analyzed the sequencing data. F.M. was involved in western blotting experiments. L. Tönges contributed to the design of the study and revised the manuscript. L. Tatenhorst participated in the animal experiments. M.B. contributed to the design of the study and interpreted the data. A.F. contributed to the design of the study, analyzed and interpreted the data, and revised the manuscript. P.L. contributed to the design of the study and its experiments, interpreted the data, and wrote the paper.

CONFLICTS OF INTEREST

The authors declare no conflict of interest.

ACKNOWLEDGMENTS

The authors thank Elisabeth Barski, Vivian Dambeck, and Sabine Ceramella for technical assistance and Dr. Sameehan Mahajani and Claudia Fokken for experimental support during the revision of this manuscript. This study was supported by the Cluster of Excellence and DFG Research Center Nanoscale Microscopy and Molecular Physiology of the Brain, Göttingen, Germany.

REFERENCES

- Dexter, D.T., and Jenner, P. (2013). Parkinson disease: from pathology to molecular disease mechanisms. *Free Radic. Biol. Med.* 62, 132–144.
- Burke, R.E., and O'Malley, K. (2013). Axon degeneration in Parkinson's disease. *Exp. Neurol.* 246, 72–83.
- Tönges, L., Frank, T., Tatenhorst, L., Saal, K.A., Koch, J.C., Szego, É.M., Bähr, M., Weishaupt, J.H., and Lingor, P. (2012). Inhibition of rho kinase enhances survival of dopaminergic neurons and attenuates axonal loss in a mouse model of Parkinson's disease. *Brain* 135, 3355–3370.
- Schratt, G. (2009). Fine-tuning neural gene expression with microRNAs. *Curr. Opin. Neurobiol.* 19, 213–219.
- Saba, R., and Schratt, G.M. (2010). MicroRNAs in neuronal development, function and dysfunction. *Brain Res.* 1338, 3–13.
- Kim, J., Inoue, K., Ishii, J., Vanti, W.B., Voronov, S.V., Murchison, E., Hannon, G., and Abeliovich, A. (2007). A MicroRNA feedback circuit in midbrain dopamine neurons. *Science* 317, 1220–1224.
- Müller, M., Kuiperij, H.B., Claassen, J.A., Küsters, B., and Verbeek, M.M. (2014). MicroRNAs in Alzheimer's disease: differential expression in hippocampus and cell-free cerebrospinal fluid. *Neurobiol. Aging* 35, 152–158.
- Zovoilis, A., Agbemenyah, H.Y., Agis-Balboa, R.C., Stilling, R.M., Edbauer, D., Rao, P., Farinelli, L., Delalle, I., Schmitt, A., Falkai, P., et al. (2011). MicroRNA-34c is a novel target to treat dementias. *EMBO J.* 30, 4299–4308.
- Miñones-Moyano, E., Porta, S., Escaramis, G., Rabionet, R., Iraola, S., Kagerbauer, B., Espinosa-Parrilla, Y., Ferrer, I., Estivill, X., and Martí, E. (2011). MicroRNA profiling of Parkinson's disease brains identifies early downregulation of miR-34b/c which modulate mitochondrial function. *Hum. Mol. Genet.* 20, 3067–3078.
- Kordower, J.H., Emborg, M.E., Bloch, J., Ma, S.Y., Chu, Y., Leventhal, L., McBride, J., Chen, E.Y., Palfi, S., Roitberg, B.Z., et al. (2000). Neurodegeneration prevented by lentiviral vector delivery of GDNF in primate models of Parkinson's disease. *Science* 290, 767–773.
- Kriegstein, K., Suter-Crazzola, C., Fischer, W.H., and Unsicker, K. (1995). TGF-beta superfamily members promote survival of midbrain dopaminergic neurons and protect them against MPP+ toxicity. *EMBO J.* 14, 736–742.
- Vo, N., Klein, M.E., Varlamova, O., Keller, D.M., Yamamoto, T., Goodman, R.H., and Impey, S. (2005). A cAMP-response element binding protein-induced microRNA regulates neuronal morphogenesis. *Proc. Natl. Acad. Sci. USA* 102, 16426–16431.
- Hsu, S.D., Tseng, Y.T., Shrestha, S., Lin, Y.L., Khaleel, A., Chou, C.H., Chu, C.F., Huang, H.Y., Lin, C.M., Ho, S.Y., et al. (2014). miRTarBase update 2014: an information resource for experimentally validated miRNA-target interactions. *Nucleic Acids Res.* 42, D78–D85.
- Guttilla, I.K., and White, B.A. (2009). Coordinate regulation of FOXO1 by miR-27a, miR-96, and miR-182 in breast cancer cells. *J. Biol. Chem.* 284, 23204–23216.
- Segura, M.F., Hanniford, D., Menendez, S., Reavie, L., Zou, X., Alvarez-Diaz, S., Zakrzewski, J., Blochin, E., Rose, A., Bogunovic, D., et al. (2009). Aberrant miR-182 expression promotes melanoma metastasis by repressing FOXO3 and microphthalmia-associated transcription factor. *Proc. Natl. Acad. Sci. USA* 106, 1814–1819.
- Gilley, J., Coffey, P.J., and Ham, J. (2003). FOXO transcription factors directly activate bim gene expression and promote apoptosis in sympathetic neurons. *J. Cell Biol.* 162, 613–622.
- Xie, Q., Hao, Y., Tao, L., Peng, S., Rao, C., Chen, H., You, H., Dong, M.Q., and Yuan, Z. (2012). Lysine methylation of FOXO3 regulates oxidative stress-induced neuronal cell death. *EMBO Rep.* 13, 371–377.
- Wang, H., Duan, X., Ren, Y., Liu, Y., Huang, M., Liu, P., Wang, R., Gao, G., Zhou, L., Feng, Z., and Zheng, W. (2013). FOXO3a negatively regulates nerve growth factor-induced neuronal differentiation through inhibiting the expression of neurochondrin in PC12 cells. *Mol. Neurobiol.* 47, 24–36.
- Yuan, Z., Lehtinen, M.K., Merlo, P., Villén, J., Gygi, S., and Bonni, A. (2009). Regulation of neuronal cell death by MST1-FOXO1 signaling. *J. Biol. Chem.* 284, 11285–11292.
- Woodbury, D., Schaar, D.G., Ramakrishnan, L., and Black, I.B. (1998). Novel structure of the human GDNF gene. *Brain Res.* 803, 95–104.
- Tanaka, M., Ito, S., and Kiuchi, K. (2000). Novel alternative promoters of mouse glial cell line-derived neurotrophic factor gene. *Biochim. Biophys. Acta* 1494, 63–74.
- He, D.-Y., and Ron, D. (2006). Autoregulation of glial cell line-derived neurotrophic factor expression: implications for the long-lasting actions of the anti-addiction drug, Ibogaine. *FASEB J.* 20, 2420–2422.
- Yang, W.-B., Chen, P.-H., Hsu, T., Fu, T.-F., Su, W.-C., Liaw, H., Chang, W.C., and Hung, J.J. (2014). Sp1-mediated microRNA-182 expression regulates lung cancer progression. *Oncotarget* 5, 740–753.
- Gómez-Villafuertes, R., García-Huerta, P., Díaz-Hernández, J.I., and Miras-Portugal, M.T. (2015). PI3K/Akt signaling pathway triggers P2X7 receptor expression as a pro-survival factor of neuroblastoma cells under limiting growth conditions. *Sci. Rep.* 5, 18417.
- Lin, L.F., Doherty, D.H., Lile, J.D., Bektess, S., and Collins, F. (1993). GDNF: a glial cell line-derived neurotrophic factor for midbrain dopaminergic neurons. *Science* 260, 1130–1132.
- Gash, D.M., Zhang, Z., and Gerhardt, G. (1998). Neuroprotective and neurorestorative properties of GDNF. *Ann. Neurol.* 44 (Suppl 1), S121–S125.
- Remenyi, J., Hunter, C.J., Cole, C., Ando, H., Impey, S., Monk, C.E., Martin, K.J., Barton, G.J., Hutvagner, G., and Arthur, J.S. (2010). Regulation of the miR-212/132 locus by MSK1 and CREB in response to neurotrophins. *Biochem. J.* 428, 281–291.

28. Terasawa, K., Ichimura, A., Sato, F., Shimizu, K., and Tsujimoto, G. (2009). Sustained activation of ERK1/2 by NGF induces microRNA-221 and 222 in PC12 cells. *FEBS J.* 276, 3269–3276.
29. Marler, K.J., Suetterlin, P., Dopplapudi, A., Rubikaite, A., Adnan, J., Maiorano, N.A., Lowe, A.S., Thompson, I.D., Pathania, M., Bordey, A., et al. (2014). BDNF promotes axon branching of retinal ganglion cells via miRNA-132 and p250GAP. *J. Neurosci.* 34, 969–979.
30. Busskamp, V., Krol, J., Nelidova, D., Daum, J., Szikra, T., Tsuda, B., Jüttner, J., Farrow, K., Scherf, B.G., Alvarez, C.P., et al. (2014). miRNAs 182 and 183 are necessary to maintain adult cone photoreceptor outer segments and visual function. *Neuron* 83, 586–600.
31. Woldemichael, B.T., Jawaid, A., Kremer, E.A., Gaur, N., Krol, J., Marchais, A., and Mansuy, I.M. (2016). The microRNA cluster miR-183/96/182 contributes to long-term memory in a protein phosphatase 1-dependent manner. *Nat. Commun.* 7, 12594.
32. Lumayag, S., Haldin, C.E., Corbett, N.J., Wahlin, K.J., Cowan, C., Turturro, S., Larsen, P.E., Kovacs, B., Witmer, P.D., Valle, D., et al. (2013). Inactivation of the microRNA-183/96/182 cluster results in syndromic retinal degeneration. *Proc. Natl. Acad. Sci. USA* 110, E507–E516.
33. Wang, W.M., Lu, G., Su, X.W., Lyu, H., and Poon, W.S. (2017). MicroRNA-182 regulates neurite outgrowth involving the PTEN/AKT pathway. *Front. Cell. Neurosci.* 11, 96.
34. Song, J., Kang, S.M., Kim, E., Kim, C.-H., Song, H.-T., and Lee, J.E. (2015). Impairment of insulin receptor substrate 1 signaling by insulin resistance inhibits neurite outgrowth and aggravates neuronal cell death. *Neuroscience* 301, 26–38.
35. Gu, T., Zhao, T., and Hewes, R.S. (2014). Insulin signaling regulates neurite growth during metamorphic neuronal remodeling. *Biol. Open* 3, 81–93.
36. Wong, H.K.A., Veremeyko, T., Patel, N., Lemere, C.A., Walsh, D.M., Esau, C., Vanderburg, C., and Krichevsky, A.M. (2013). De-repression of FOXO3a death axis by microRNA-132 and -212 causes neuronal apoptosis in Alzheimer's disease. *Hum. Mol. Genet.* 22, 3077–3092.
37. Ryu, H., Lee, J., Olofsson, B.A., Mwida, A., Dedeoglu, A., Escudero, M., Flemington, E., Azizkhan-Clifford, J., Ferrante, R.J., and Ratan, R.R. (2003). Histone deacetylase inhibitors prevent oxidative neuronal death independent of expanded polyglutamine repeats via an Sp1-dependent pathway. *Proc. Natl. Acad. Sci. USA* 100, 4281–4286.
38. Tomac, A., Lindqvist, E., Lin, L.F., Ogren, S.O., Young, D., Hoffer, B.J., and Olson, L. (1995). Protection and repair of the nigrostriatal dopaminergic system by GDNF *in vivo*. *Nature* 373, 335–339.
39. Pore, N., Liu, S., Shu, H.-K., Li, B., Haas-Kogan, D., Stokoe, D., Milanini-Mongiat, J., Pages, G., O'Rourke, D.M., Bernhard, E., and Maity, A. (2004). Sp1 is involved in Akt-mediated induction of VEGF expression through an HIF-1-independent mechanism. *Mol. Biol. Cell* 15, 4841–4853.
40. Bae, I.H., Park, M.-J., Yoon, S.H., Kang, S.W., Lee, S.-S., Choi, K.-M., and Um, H.D. (2006). Bcl-w promotes gastric cancer cell invasion by inducing matrix metalloproteinase-2 expression via phosphoinositide 3-kinase, Akt, and Sp1. *Cancer Res.* 66, 4991–4995.
41. Marinova, Z., Ren, M., Wendland, J.R., Leng, Y., Liang, M.-H., Yasuda, S., Leeds, P., and Chuang, D.M. (2009). Valproic acid induces functional heat-shock protein 70 via Class I histone deacetylase inhibition in cortical neurons: a potential role of Sp1 acetylation. *J. Neurochem.* 111, 976–987.
42. Deng, X., Zhang, W., O'Sullivan, I., Williams, J.B., Dong, Q., Park, E.A., Raghow, R., Unterman, T.G., and Elam, M.B. (2012). FoxO1 inhibits sterol regulatory element-binding protein-1c (SREBP-1c) gene expression via transcription factors Sp1 and SREBP-1c. *J. Biol. Chem.* 287, 20132–20143.
43. van Rooij, E., Purcell, A.L., and Levin, A.A. (2012). Developing microRNA therapeutics. *Circ. Res.* 110, 496–507.
44. Lingor, P., Unsicker, K., and Kriegstein, K. (1999). Midbrain dopaminergic neurons are protected from radical induced damage by GDF-5 application. *Short communication. J. Neural Transm. (Vienna)* 106, 139–144.
45. Lewis, B.P., Burge, C.B., and Bartel, D.P. (2005). Conserved seed pairing, often flanked by adenosines, indicates that thousands of human genes are microRNA targets. *Cell* 120, 15–20.
46. Huang, W., Sherman, B.T., and Lempicki, R.A. (2009). Systematic and integrative analysis of large gene lists using DAVID bioinformatics resources. *Nat. Protoc.* 4, 44–57.
47. Papadopoulos, G.L., Alexiou, P., Maragkakis, M., Reczko, M., and Hatzigeorgiou, A.G. (2009). DIANA-mirPath: integrating human and mouse microRNAs in pathways. *Bioinformatics* 25, 1991–1993.
48. Saal, K.-A., Koch, J.C., Tatenhorst, L., Szegő, E.M., Ribas, V.T., Michel, U., Bähr, M., Tönges, L., and Lingor, P. (2015). AAV.shRNA-mediated downregulation of ROCK2 attenuates degeneration of dopaminergic neurons in toxin-induced models of Parkinson's disease *in vitro* and *in vivo*. *Neurobiol. Dis.* 73, 150–162.
49. Zala, D., Hinckelmann, M.-V., Yu, H., Lyra da Cunha, M.M., Liot, G., Cordelières, F.P., Marco, S., and Saudou, F. (2013). Vesicular glycolysis provides on-board energy for fast axonal transport. *Cell* 152, 479–491.
50. Alvarez-Fischer, D., Henze, C., Strenzke, C., Westrich, J., Ferger, B., Höglinger, G.U., Oertel, W.H., and Hartmann, A. (2008). Characterization of the striatal 6-OHDA model of Parkinson's disease in wild type and α -synuclein-deleted mice. *Exp. Neurol.* 210, 182–193.
51. Paxinos, G., and Franklin, K.B.J. (2004). *The Mouse Brain in Stereotaxic Coordinates* (Elsevier Science).
52. Schallert, T., Fleming, S.M., Leasure, J.L., Tillerson, J.L., and Bland, S.T. (2000). CNS plasticity and assessment of forelimb sensorimotor outcome in unilateral rat models of stroke, cortical ablation, parkinsonism and spinal cord injury. *Neuropharmacology* 39, 777–787.

Supplemental Information

**miR-182-5p and miR-183-5p Act as GDNF Mimics
in Dopaminergic Midbrain Neurons**

**Anna-Elisa Roser, Lucas Caldi Gomes, Rashi Halder, Gaurav Jain, Fabian Maass, Lars
Tönges, Lars Tatenhorst, Mathias Bähr, André Fischer, and Paul Lingor**

Supplemental information

Supplemental figures

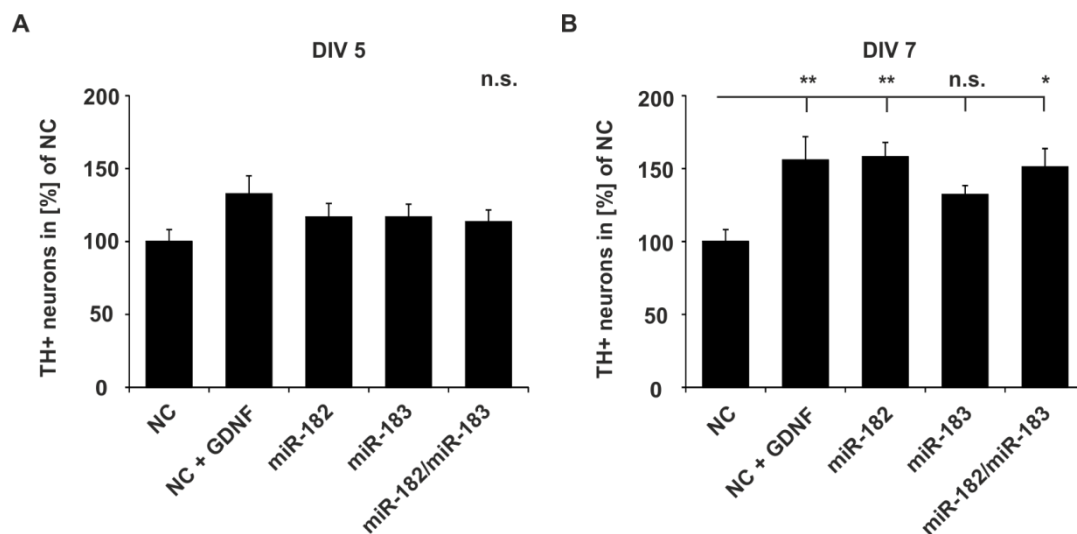


Figure S1 – Effects on DA neuron survival at DIV 5 and DIV 7 (Corresponding to Fig 3).

A+B Relative quantification of surviving TH+ PMNs after transfection with miR mimic, NC or treatment with GDNF at DIV 5 (A) and DIV 7 (B) normalized to NC ($n = 3-5$) independent experiments). Data are presented as mean \pm SEM and were analyzed by one way ANOVA with Dunnett's post-hoc test. * $P < 0.05$, ** $P < 0.01$.

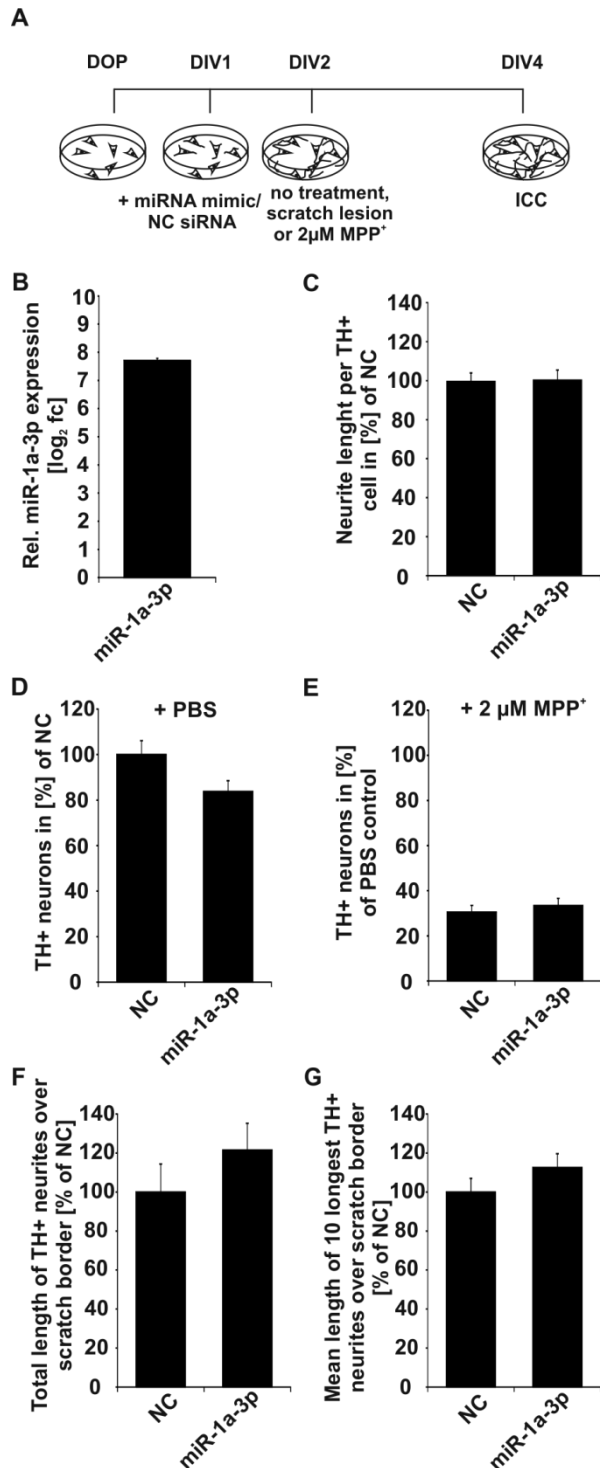


Figure S2 – Effects on neuronal survival and neurite growth are not caused by an increase in miRNA levels per se (Corresponding to Fig 2+3).

A Experimental layout for miR-1a-3p experiments.

B Relative miR-1a-3p level in cultures transfected with miR-1a-3p mimic normalized to NC transfected cultures ($n = 3$ independent cultures).

C Quantification of neurite length of dopaminergic PMNs transfected with miR-1a-3p mimic or NC ($n = 3$ independent cultures).

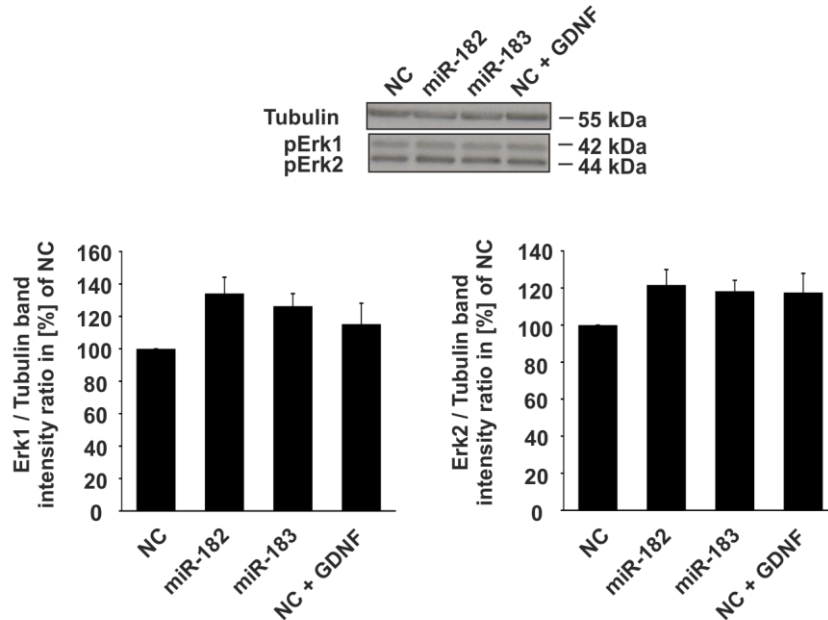
D Quantification of TH+ PMNs after transfection with miR-1a-3p mimics or NC and with addition of PBS for 24 h as experimental control.

E Relative quantification of surviving TH+ PMNs after transfection with miR-1a-3p mimics or NC and addition of 2 µM MPP⁺ for 24 h normalized to PBS treated cells ($n = 3$ independent cultures).

F Quantification of total length of TH+ neurites growing over the scratch border relative to NC transfected PMNs ($n = 3$ independent cultures).

G Quantification showing the mean length of the 10 longest TH+ neurites crossing the scratch border relative to NC transfected cultures ($n = 3$ independent cultures). Data are given as mean \pm SEM and analyzed by one-way ANOVA.

A



B

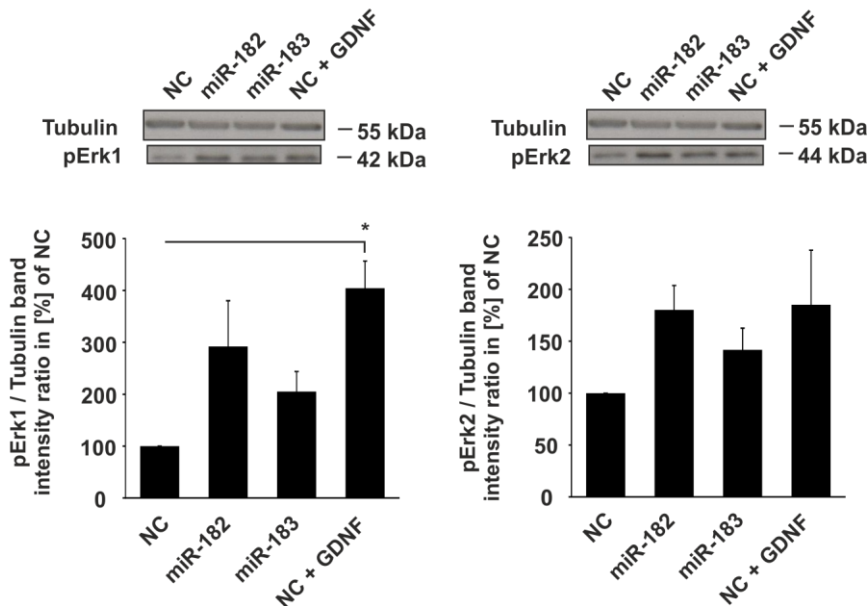


Figure S3 – Effects of miR-182-5p and miR-183-5p increase and GDNF treatment on MAPK signaling in PMNs (Corresponding to Fig 5).

A+B Western blot analyses for **A** Erk1 and Erk2 ($n = 4$ independent experiments) and **B** pErk1 (left; $n = 4$ independent experiments) and pErk2 (right; $n = 4$ independent experiments). Data are presented as mean \pm SEM and were analyzed by one way ANOVA with Dunnett's post-hoc test. * $P < 0.05$.

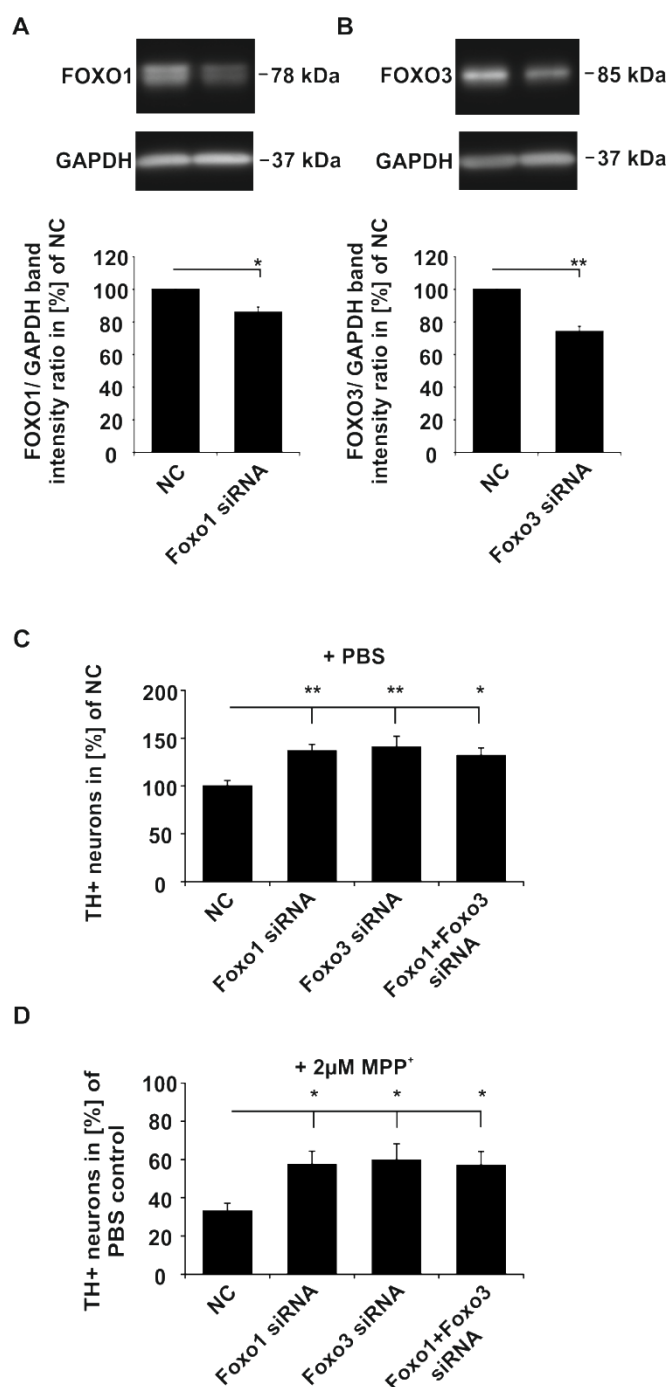


Figure S4 – Decrease in FOXO1 and FOXO3 levels lead to a higher DA neuron survival in PMN cultures (Corresponding to Fig 5).

A+B Relative FOXO1 (left) and FOXO3 (right) protein levels in PMN cultures transfected with Foxo1 and/ or Foxo3 siRNA normalized to NC transfected cultures ($n = 5$ independent cultures). Data are presented as mean \pm SEM and were analyzed by one way ANOVA with Dunnett's post-hoc test. * $P < 0.05$, ** $P < 0.01$.

C Quantification of TH+ PMNs after transfection with Foxo1 and/ or Foxo3 siRNA or NC and with addition of PBS for 24 h as experimental control.

D Relative quantification of surviving TH+ PMNs after transfection with Foxo1 and/ or Foxo3 siRNA or NC and addition of 2 μ M MPP⁺ for 24 h normalized to PBS treated cells ($n = 5$ independent cultures). Data are presented as mean \pm SEM and were analyzed by one way ANOVA with Dunnett's post-hoc test. * $P < 0.05$.

Supplemental tables

Table S1 - Differential expression analysis small RNA sequencing.

Differential expression analyses comparing miR expression levels between DIV 1 and DIV 5 (during development), the effect of GDNF-treatment at DIV 1 and the effect of GDNF-treatment at DIV 5 (Corresponding to Fig 1). Separate excel file.

Table S2 – Gene ontology (GO) and KEGG-pathway enrichment analyses for predicted miR-182-5p and miR-183-5p target genes (Corresponding to Fig 1).

A

Functional annotation of miR-182 targets			Functional annotation of miR-183 targets		
#	GO: Biological process	p-value	#	GO: Biological process	p-value
1	Cell motion	6.30E-10	1	Homophilic cell adhesion	3.50E-09
2	Cell projection organization	3.50E-09	2	Cell-cell adhesion	8.40E-07
3	Neuron projection development	5.90E-08	3	Cell adhesion	6.70E-06
4	Cell morphogenesis involved in neuron differentiation	6.80E-08	4	Biological adhesion	6.90E-06
5	Neuron development	1.20E-07	5	Phosphate metabolic process	2.90E-05
#	GO: Panther database: Biological process	p-value	#	GO: Panther database: Biological process	p-value
1	BP00199:Neurogenesis	3.90E-09	1	BP00124:Cell adhesion	3.90E-09
2	BP00246:Ectoderm development	5.20E-08	2	BP00242:Embryogenesis	5.20E-08
3	BP00063:Protein modification	5.40E-07	3	BP00064:Protein phosphorylation	5.40E-07
4	BP00111:Intracellular signaling cascade	1.10E-06	4	BP00285:Cell structure and motility	1.10E-06
5	BP00111:Intracellular signaling cascade	6.40E-06	5	BP00120:Cell adhesion-mediated signaling	6.40E-06
#	KEGG pathway	p-value	#	KEGG pathway	p-value
1	Long-term depression	8.51E-08	1	Transcriptional misregulation in cancer	5.13E-08
2	Neurotrophin signaling pathway	7.24E-06	2	Other glycan degradation	1.38E-05
3	Bacterial invasion of epithelial cells	7.27E-06	3	Wnt signaling pathway	3.25E-05
4	Oocyte meiosis	5.06E-05	4	Dopaminergic synapse	3.43E-05
5	Long-term potentiation	5.06E-05	5	Tight junction	5.12E-09